# Formation of a Fast Charge Transfer Channel in Quasi-2D Perovskite Solar Cells through External Electric Field Modulation

Xixiang Zhu [1,3], Liping Peng [2], Jinpeng Li [1], Haomiao Yu [1] and Yulin Xie [2,*]

1   Key Laboratory of Luminescence and Optical Information, Department of Physics, School of Science, Beijing Jiaotong University, Ministry of Education, Beijing 100044, China; xxzhu@bjtu.edu.cn (X.Z.); jinpengli@bjtu.edu.cn (J.L.); yuhaomiao@bjtu.edu.cn (H.Y.)
2   School of Physics and Electronics, Huanggang Normal University, Huanggang 438000, China; pengliping@hgnu.edu.cn
3   School of Electronic and Information Engineering, Beijing Jiaotong University, Beijing 100044, China
*   Correspondence: xieyulin@hgnu.edu.cn

**Abstract:** Quasi-2D perovskites solar cells exhibit excellent environmental stability, but relatively low photovoltaic properties, compared with 3D perovskites solar cells. However, charge transport and extraction in quasi-2D perovskite solar cells are still limited by the inevitable quantum well effect, resulting in low power conversion efficiency (PCE). To date, most efforts concentrate on crystal orientation and favorable alignment during materials and films processing. In this paper, we demonstrated that the quasi-2D perovskite $[(BA)_2(MA)_3Pb_4I_{13}$ ($n$ = 4)] solar cells show an optimized device performance through forming a fast charge transfer channel among 2D quantum wells through external electric field modulation, with appropriate modulation bias and time after the device has been fabricated. Essentially, ions will move directionally due to local polarization in quasi-2D perovskite solar cells under the action of electric field modulation. More importantly, the mobile ions function as a dopant to de-passivate the defects when releasing at grain boundaries, while decreasing built-in potential by applying forward modulation bias with proper modulation time. The capacitance-voltage characteristics indicate that electric field modulation can decrease the charge accumulation and improve the charge collection in quasi-2D perovskite solar cells. Photoluminescence (PL) studies confirm that the non-radiative recombination is reduced by electric field modulation, leading to enhanced charge transfer. Our work indicates that external electric field modulation is an effective method to form a fast charge transfer channel among 2D quantum wells, leading to enhanced charge transfer and charge collection through local polarization toward developing high–performance quasi-2D perovskite devices.

**Keywords:** quasi-2D perovskite; ions; electric field modulation

## 1. Introduction

Quasi-2D perovskite solar cells have shown great potential in future photovoltaic applications, due to their tunable energy level and comparable stability [1–7]. Basically, quasi-2D perovskites are prepared with the Ruddlesden–Popper perovskite (RPP) nanoplates structures, which has been an effective method for enhancing the stability for photovoltaic applications [8–10]. Due to the disconnected inorganic semiconducting network in the direction of the spacing cations in the RPP structure, the charge carrier transport is drastically limited, decreasing the photocurrent in quasi-2D perovskites solar cells [11,12]. Recent studies have introduced 2D perovskite nanoplates processing methods, such as hot-casting or vacuum fabrication method, to orient 2D perovskites preferentially in the out-of-plane direction, where the 2D nanoplates can efficiently connect the electron and hole selective electrode layers with improved charge carrier transport and device performance [12–14]. Furthermore, the layered structure of low-dimensional perovskite can effectively inhibit ion migration, thereby reducing the degradation of perovskite caused by ion diffusion

or the corrosion in charge transport, which is beneficial to improve the stability of perovskite [15–17]. Nevertheless, ion migration still exists in such quasi-2D perovskites. It becomes the main reason that causes the device to have a hysteresis effect, giving rise to the impact on charge carrier transfer or energy transfer between 2D quantum wells [18–20]. It should be noted that the hysteresis effect caused by exogenous ions may even be more substantial than intrinsic ions [21,22]. Moreover, electric field modulation is a crucial method to explore the migration of perovskite ions [23–25]. Recently, PL studies indicated that charge-transfer excitons can be formed at the interface within 2D perovskite heterostructures to realize a broad light emission [26]. Therefore, exploring the external electric field modulation effect on the detailed charge carrier dynamics and the corresponding RPPs structural correlation of quasi-2D perovskites involved in internal photovoltaic processes remains valuable, and is essential to achieve more useful photogenerated carriers.

To date, a lot of work reported the performance of 2D perovskite solar cells could be improved through film or materials processing. However, it is rarely reported on the use of methods to further improve device performance after the device has been fabricated. In this work, we develop a simple and effective method to enhance the charge transfer among 2D quantum wells in quasi-2D perovskite solar cells, with the aim of further improving the PCE after the device has been fabricated. A quasi-2D perovskite [$(BA)_2(MA)_3Pb_4I_{13}$ ($n = 4$)] solar cell was prepared by changing the preheating temperature, and annealing temperature of the perovskite layer. We should note that even the enhanced charge transport/extraction and final power conversion efficiency (PCE) in $BA_2MA_3Pb_4I_{13}$ based quasi-2D perovskite solar cells benefit from efforts to change the vertical arrangement of the BA spacer cations, and the impact of quantum wells is still inevitable, and even under optimal conditions, it will cause the electrical field-dependent charge extraction and fill factor (FF) reduction in the quasi-2D perovskite solar cell [27]. Here, we found that a fast charge transfer channel can be formed among 2D quantum wells by applying external electric field modulation with forwarding bias at a constant time through local electric polarization in quasi-2D perovskite solar cells. By combining capacitance-voltage ($C–V$) and PL characteristics studies, we demonstrate that fast charge transfer can be ascribed to the enhanced built-in potential due to passivation of defects at grain boundaries, while decreasing built-in potential by applying forward bias through enhanced local polarization. Importantly, revealing the effects of electric field modulation on the charge transport/collection and recombination provides a constructive scheme of quasi-2D perovskites solar cells toward further promoting photovoltaic properties.

## 2. Materials and Methods

### 2.1. Material Processing and Device Fabrication

The quasi-2D solar cells were prepared in the p-i-n structure of the ITO/PEDOT:PSS/$(BA)_2MA_3Pb_4I_{13}$/ PCBM/ PEI/ Ag preheating method to explore the effects of electric field modulation on device performance. The perovskite precursor comprised $PbI_2$ (99.999%, Sigma-Aldrich, St. Louis, MO, USA), MAI (99%, Shanghai Materwin, Shanghai, China), and BAI (99.5%, Xi'an Polymer, Xi'an, China), with a 4:3:2 molar ratio in a mixed solvent of N,N–dimethylformamide (DMF, 99.9%, Alfa Aesar, Ward Hill, MA, USA) and dimethyl sulfoxide (DMSO, 99.9%, Sigma–Aldrich) in 9:1 volume with a concentration of 0.8 M. Before coating, the indium tin oxides glass (ITO) glass substrates were cleaned and then exposed to plasma for 5 min. The hole transporting layer poly(3,4-ethylenedioxythiophene) poly(styrenesulfonate) (PEDOT:PSS) 4083 (Xi'an Polymer) was coated on ITO at 4000 rpm for 40 s, and then dried in an oven at 120 °C for 30 min. Before covering the perovskite film, the ITO/ PEDOT:PSS substrates were preheated on a hot plate at 100 °C for 3–5 min. Then, the regulated perovskite solution was deposited by dropping 40 μL on the ITO/ PEDOT:PSS substrates at 5000 rpm for 30 s. The as-coated sample was dried at 100 °C for 10 min. The electron transport layer PCBM (Lumtech, 99.5%, Moorestown, NJ, USA) was dissolved in chlorobenzene (Sigma–Aldrich, 99.8%), and coated on the perovskite film at 2000 rpm for 45 s at a concentration of 20 mg/mL. The

PEI (0.1 wt % in isopropanol) was spin-coated at 5000 rpm for 50 s. Finally, a 100 nm silver electrode was evaporated on the substrates under a pressure of $3 \times 10^{-4}$ Pa, and the active area of all devices was 0.055 cm$^2$.

### 2.2. Device Characterization

The device performances (*J*–*V* curves) were obtained using a Newport Thermal Oriel 96000 with Keithley 2400 under the illumination of 1 sun with a 20 mV s$^{-1}$ scan rate in air. The morphology of quasi-2D perovskite films were observed with a Bruker Dimension 3100 and Quanta 3D FEG-FIB. The luminescence spectrum was recorded with an Edinburgh FLS920. A HORIBA Scientific DeltaPro was used to record the PL of the quasi-2D perovskite. An Agilent 4294A impedance spectroscopy analyzer was used to record *C*–*V* spectra at a dark state.

## 3. Results

### 3.1. Device Section

The *J*–*V* characteristic curves of quasi-2D solar cells are shown in Figure 1a, with different preheating temperatures under AM 1.5 G are measured using forward and reversed scan, and the corresponding photovoltaic parameters are shown in Table 1. Among them, 0 V bias is the original device without any external electric field.
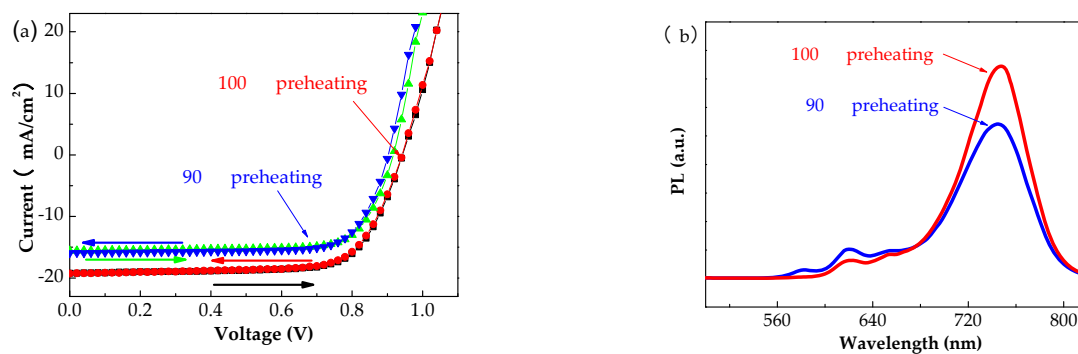


**Figure 1.** (**a**) *J*–*V* curve of quasi-2D perovskite [(BA)$_2$MA$_3$Pb$_4$I$_{13}$, *n* = 4] solar cells processing with preheating of 90 °C and 100 °C under forward and reversed scan. (**b**) PL spectra of perovskite films from front sides at 90 °C and 100 °C preheating temperatures.

**Table 1.** Photovoltaic parameters of electric field modulated quasi-2D perovskite solar cells under different modulation bias at 200 s with the same batch of devices.

| Modulation Bias | $V_{OC}$ (V) | $J_{SC}$ (mA·cm$^{-2}$) | FF (%) | PCE (%) |
|---|---|---|---|---|
| 0 V | 1.03 | 20.14 | 63.89 | 13.2 |
| 0.8 V | 1.04 | 20.28 | 63.69 | 13.45 |
| 1.0 V | 1.04 | 20.06 | 63.57 | 13.27 |
| 1.5 V | 1.10 | 19.22 | 59.03 | 12.48 |
| −0.1 V | 1.10 | 18.11 | 63.00 | 12.55 |
| −0.5 V | 0.87 | 18.48 | 32.97 | 5.27 |

Clearly, the photocurrent hysteresis of all devices can be ignored. It can be seen that the higher efficiency of 13.2% ($V_{OC}$ = 0.94 V, $J_{SC}$ = 19.24 mA·cm$^{-2}$, FF = 0.73) is obtained when using 100 °C to preheat the PEDOT:PSS samples, as compared with the devices without 90 °C preheating PCE = 10.8% ($V_{OC}$ = 0.92 V, $J_{SC}$ = 15.6 mA·cm$^{-2}$, FF = 0.75). We also note that when the PL spectra of quasi-2D perovskites is under the preheating condition of 100 °C, the main peak of PL intensity of the quasi-2D perovskite film is greater than that of the quasi-2D perovskite film under the preheating condition of 90 °C (Figure 1b). This indicates that increasing the preheating temperature can promote the radiative recombination luminescence of the quasi-2D perovskite (Figure S1). The corresponding mobility of

the device is $6.3 \times 10^{-3}$ cm$^2 \cdot$V$^{-1} \cdot$s$^{-1}$ under the illumination of 0.54 mW$\cdot$cm$^{-2}$, measured from the charge extraction by linear increasing voltage (CELIV) method (Figure S2).

### 3.2. AFM Methodology

Morphology is an important parameter that affects device performance. Figure 2a shows the morphology of 2D perovskite films; when preheating at 90 °C, the surface morphology of perovskite shows partial cracks and small grain size, indicating that there are many defects on the surface of quasi-2D perovskites prepared under preheating at 90 °C and uneven film formation, which will reduce the photovoltaic efficiency of 2D perovskite solar cells. When the preheating temperature is increased to 100 °C, the perovskite crystallizes well, and the grain size becomes larger and compact (Figure 2a,b). The better crystallization of perovskite can inhibit migration and enhance charge transmission and collection.



(**a**)                                                    (**b**)
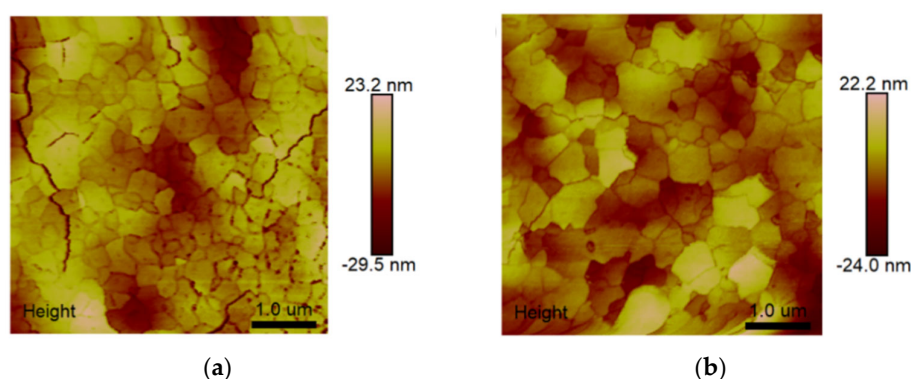
**Figure 2.** Surface morphology of $(BA)_2MA_3Pb_4I_{13}$ with (**a**) preheating at 90 °C and (**b**) preheating at 100 °C.

### 3.3. Signal Analysis (Electric Field Modulation and Impedance Spectra Analysis)

Now, we discuss the charge transfer of quasi-2D perovskite solar cells by electric field modulation. It is known that, under the action of the external electric field, ions will move in a directional way, which affects the charge transfer process of perovskite devices. Essentially, using proper external electric field modulation presents a new approach to improve the charge transfer between quantum wells and quasi-2D perovskite solar cells, as schematically illustrated in Figure 3. Here, the photovoltaic performance of quasi-2D perovskites is monitored by applying forward or reversed bias with different modulation times.

The *J*–*V* curve under applied other modulation times is shown in Figure 4a, a forward bias at a constant time of 200 s. When +0.8 V bias was applied, the devices yielded a high PCE of 13.45%, deriving from a $J_{SC}$ of 20.28 mA cm$^2$, an FF of 63.69%, and a $V_{OC}$ of 1.04 V. The photovoltaic parameters of quasi-2D perovskite devices were gradually reduced, along with the applied forward bias increment, indicating that ions movement would affect the charge transfer process of quasi-2D perovskite solar cells. The photovoltaic parameters are improved when the used forward bias $V_{app}$ is less than the built-in potential ($V_{bi}$); when $V_{app} > V_{bi}$, $V_{OC}$ increases, $J_{SC}$ and PCE decreases. Essentially, the quasi-2D perovskite solar cells can generate a built-in electric field to cause the directional movement of charge, and facilitate the separation of charge carriers. The shielding electric field will enhance the local polarization in quasi-2D perovskite solar cells, leading to the directional movement of ions under the action of the external electric field. Due to the shielding effect of the electric field, the charge carrier diffusion at the interface will weaken or even disappear, and the shielding electric field generated will also disappear. However, suppose that the forward bias is too large, and the charge carrier begins to be injected. In that case, the effect of shielding electric fields will be weakened, leading to a decrease in device performance [28]. Interestingly, the efficiency of quasi-2D perovskites solar cells

are decreased by applying reversed bias, as shown in Figure 4b. It can be seen that when the reversed bias voltage of −0.1 V is applied, $V_{OC}$ increases, but the device performance decreases. Moreover, $V_{OC}$ and FF decrease, obviously, and the PCE significantly reduced by decreasing the reversed bias to −0.5 V. When the reversed bias is applied, I⁻ moves towards the Ag electrode and reacts with it, leading to the enhanced ion migration and destruction of the region corresponding to the reversed bias electrode, weakening the device performance [29]. The corresponding photovoltaic parameters under forwarding or reversed bias at a constant time are summarized in Table 1. In the same modulation voltage of 2 V, the effect of different modulation times on device performance is shown in Figure 4c. The corresponding photovoltaic parameters are shown in Table 2.
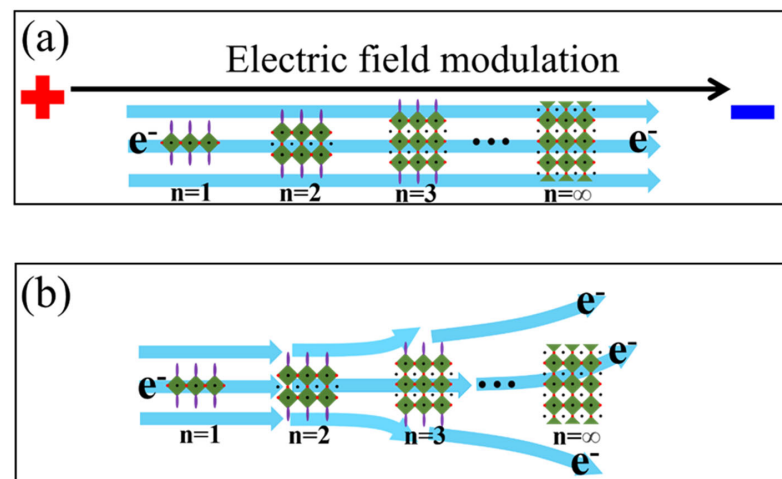


**Figure 3.** Schematic of (**a**) fast charge transfer channel between quantum wells through external electric field modulation in quasi-2D perovskite solar cells. (**b**) Inefficient random charge transfer in quasi-2D perovskite solar cells.
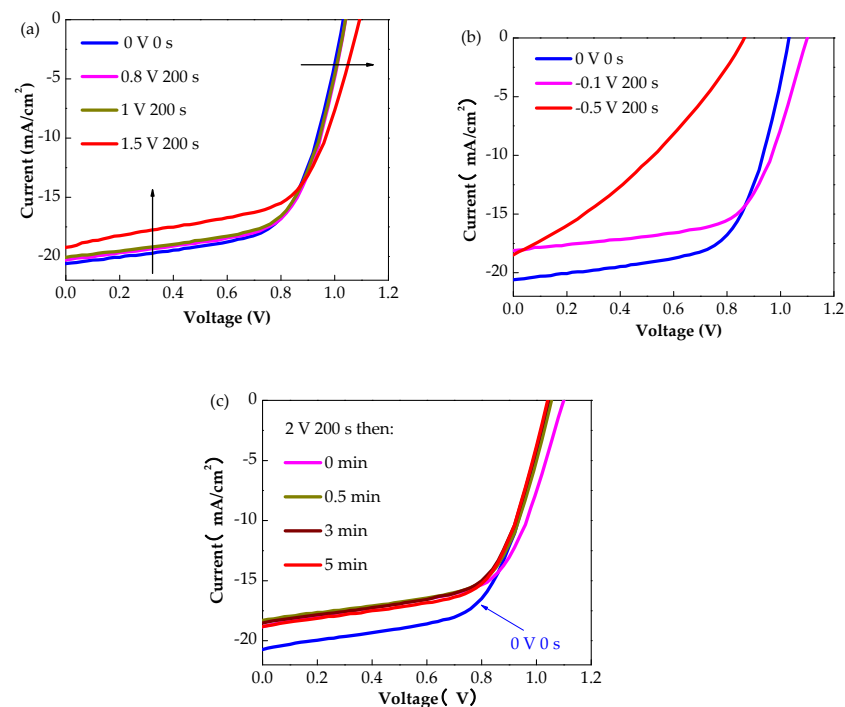


**Figure 4.** *J*–*V* curve of quasi-2D perovskite [(BA)$_2$MA$_3$Pb$_4$I$_{13}$, $n$ = 4] solar cells under external electric field modulation with (**a**) different forward bias at constant time of 200 s. (**b**) Other reversed bias at a continuous time of 200 s. (**c**) Other modulation times at consistent forward bias of 2 V.

**Table 2.** Photovoltaic parameters of electric field-modulated quasi-2D perovskite solar cells under different modulation times, at a constant forward bias with the same batch of devices.

| Modulation Bias | Time (Second) | $V_{OC}$ (V) | $J_{SC}$ (mA·cm$^{-2}$) | FF (%) | PCE (%) |
|---|---|---|---|---|---|
| 0 V | 0 s | 1.03 | 20.14 | 63.89 | 13.20 |
| | 200 s | 1.10 | 18.82 | 59.89 | 12.40 |
| 2 V | 230 s | 1.06 | 18.30 | 62.51 | 12.07 |
| | 380 s | 1.04 | 18.52 | 62.06 | 12.00 |
| | 500 s | 1.04 | 18.82 | 62.26 | 12.20 |

The quasi-2D perovskite solar cells demonstrate a worse performance by adding 2 V positive bias and a longer modulation time. We should note that the $V_{OC}$ can quickly be recovered to its initial value, but the efficiency could not be restored. When 2 V bias modulation is applied again for 20 s, both the $V_{OC}$ and PCE can be improved (Table 3). In addition, after the device is placed in the glove box with a pure nitrogen environment for 24 h, the PCE can be restored to the initial level (Table 3) [30].

**Table 3.** Photovoltaic parameters of electric field modulated quasi-2D perovskite solar cells placed in the glove box with a pure nitrogen environment after electric field modulation for 1min and 24 h with the same batch of devices.

| Modulation Bias | Restore Time | $V_{OC}$ (V) | $J_{SC}$ (mA·cm$^{-2}$) | FF (%) | PCE (%) |
|---|---|---|---|---|---|
| 2 V | 20 s | 1.12 | 17.7 | 62.25 | 12.34 |
| 0 | 24 h | 1.06 | 20.37 | 63.77 | 13.75 |

The effect of external electric field modulation on the internal electric field of the device can be analyzed according to the impedance spectrum. As shown in Figure 5a, the device capacitance peak will shift to the right when applying a forward bias of 1.5 V for 200 s, and the corresponding capacitance peak will also increase significantly. This indicates that the internal electric field reduced using electric field modulation, leading to the weakening of electric polarization and surface charge, and the increase in total charge, namely, the rise of device capacitance. Figure 5b show the $C^{-2}$-$V$ relationship and the profiles exhibit the typical Mott–Schottky behavior for the quasi-2D perovskite solar cells. The values of $V_{bi}$ can be derived via a straight-line fitting to the Mott–Schottky curve by the relationship (1):

$$C^{-2} = \frac{2}{A^2 q \varepsilon \varepsilon_0 N_A}(V_{bi} \; V_{app}) \tag{1}$$

where $q$ is the elementary charge [31,32]. By linear fitting of $C^{-2}$-$V$ curve, the $V_{bi}$ of the device without and with modulation is 1.0 V and 1.2 V, respectively. The results are consistent with the $V_{OC}$ in $J$–$V$ curve, which further indicates that the forward bias of 0.8 V for 200 s can inhibit the ion migration, and enhance the charge transfer of quasi-2D perovskite solar cells.
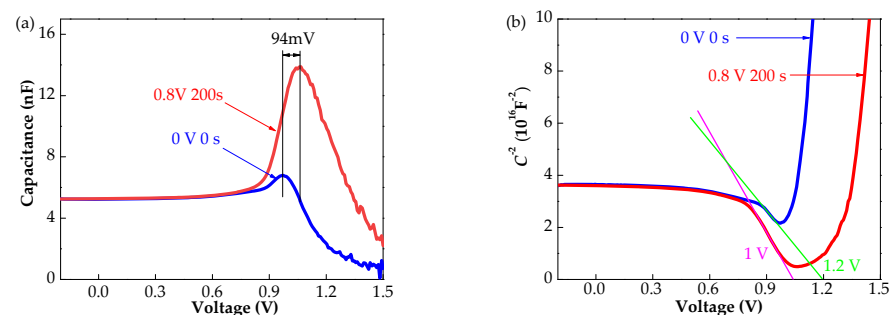


**Figure 5.** Impedance spectrum of electric field modulated quasi-2D perovskite solar cells (**a**) The $C$–$V$ spectra. (**b**) The corresponding Mott–Schottky ($C^{-2}$-$V$) curves.

## 4. Discussion

We now discuss the effect of external electric field modulation on charge transfer between quantum wells in quasi-2D perovskite solar cells using the PL method. When the external conditions are changed, such as photoexcitation and electric field modulation, the peak position and intensity of the PL spectrum will change due to ion migration, specifically, because ion migration, $MA^+$, or $I^-$ in perovskites will gradually accumulate, resulting in obvious PL quenching. Figure 6a exhibits the PL spectrum of quasi-2D perovskite solar cells with increased forward bias at constant time of 60 s. When $V_{bias}$ = 0.8 V, that is, $V_{bias} < V_{bi}$, the PL emission intensity becomes stronger, indicating that the radiative recombination emission of the quasi-2D perovskite becomes stronger under this condition, and the corresponding non-radiative recombination emission becomes weaker, which can generate more charge carriers. However, when $V_{bias} > V_{bi}$, the PL emission intensity becomes negligible, indicating that the non-radiative recombination suppresses the generation and transport of charge carriers. Interestingly, the quasi-2D perovskite solar cells can be restored to the original state after being placed in a glove box or dark environment for a period of time after the cancellation of modulation. In order to further explore the role of the external electric field modulation between different-*n*-value nanoplates in the quasi-2D perovskites solar cells, we started with the characterization for the same devices using the $\Delta PL/PL_0$ method. Here, the $\Delta PL/PL_0$ is defined by Equation (2):

$$\Delta PL \, / \, PL_0 \;=\; \frac{PL_1 - PL_0}{PL_0} \tag{2}$$

where $PL_0$ And $PL_1$ are the PL intensities without and with electric field modulation, respectively. In general, quasi-2D perovskites are normally formed with different-*n*-value nanoplates through crystallization [33,34]. The energy transfer between different-*n*-value nanoplates is the key issue determining the optical properties in 2D perovskites. We should also note that energy transfer relies on carrier transport in quasi-2D perovskite films. Essentially, PL quenching can effectively reflect the recombination process in quasi-2D perovskites. Therefore, $\Delta PL/PL_0$ can be used to study charge transport between different-*n*-value nanoplates in quasi-2D perovskite solar cells under working conditions. Here, when applied bias of 0.8 V, the $\Delta PL/PL_0$ of small *n* value become negligible. On the contrary, the $\Delta PL/PL_0$ of small *n* value peak become appreciable when the electric field modulation increases to 1.5 V and 2 V (Figure 6b). Our negligible and appreciable $\Delta PL/PL_0$ of small *n* value with and without proper forward bias further supports that electric field modulation can effectively control the charge transfer between different-*n*-value nanoplates. Figure 6c shows the PL spectra of quasi-2D perovskites under a different reversed bias. When the modulation bias is set to −0.1 V and −0.5 V, the PL spectra of devices quench rapidly, indicating that the radiative recombination luminescence of devices becomes weaker, the corresponding non-radiative recombination becomes stronger, and suppress the charge transfer between different-*n*-value nanoplates. Figure 6d demonstrates the $\Delta PL/PL_0$ curve with reversed bias, the negligible $\Delta PL/PL_0$ of small *n* value further indicates the PL intensity rapid quenching give rise to inhibits the transport of the charge carrier. The trend of PL studies is consistent with the *J-V* results of the device under reversed bias.

Moreover, The PL characteristics of the devices with the same modulation bias but different modulation time is also analyzed. Figure 7a shows the steady-state PL spectra of the devices after 0 min, 3 min, 5 min, 7 min, 10 min, and 30 min, respectively. With the increase of modulation time, the PL intensity becomes stronger, which indicates the non-radiative recombination of the devices becomes weaker. Furthermore, when reversed modulation bias of −0.5 V is applied, the PL intensity increased with modulation time, indicating that, under the reversed bias with the same direction as the $V_{bi}$, the charge carrier recombination is enhanced, leading to enhanced radiative recombination (Figure 7b). Clearly, our results indicate that the external electric field modulation is indeed responsible for forming fast charge transfer channel between quantum wells quasi-2D perovskite solar cells.
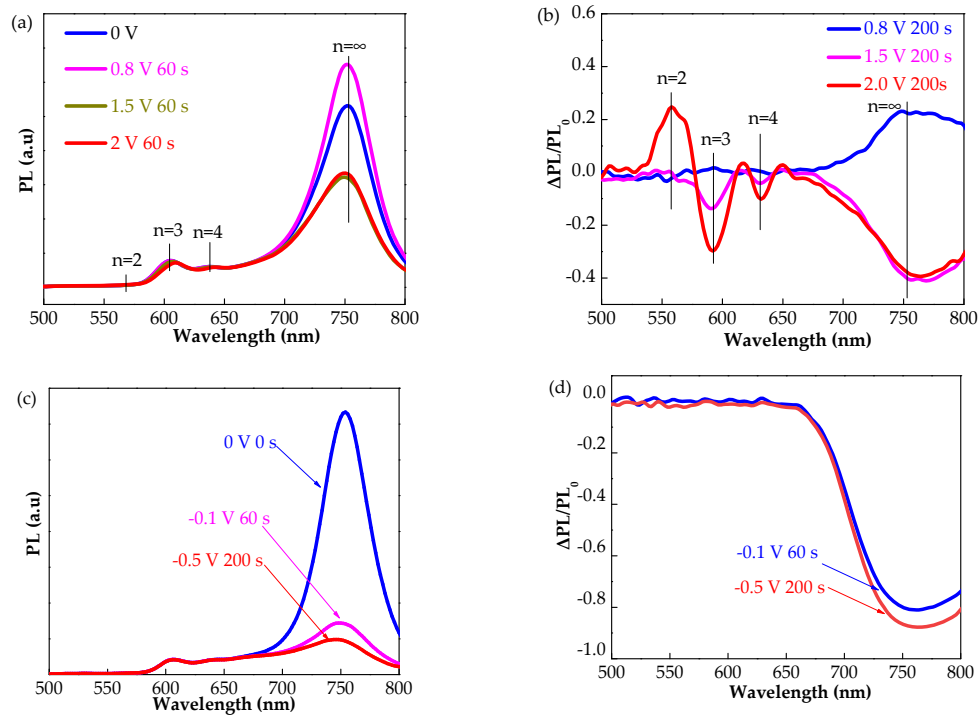
**Figure 6.** Optical characteristic spectra of electric field modulated quasi-2D perovskite solar cells. Under different, forward bias at constant time: (**a**) PL spectra. (**b**) $\Delta PL/PL_0$ curve. Under other reversed bias with vary time: (**c**) PL spectra. (**d**) $\Delta PL/PL_0$ curve.
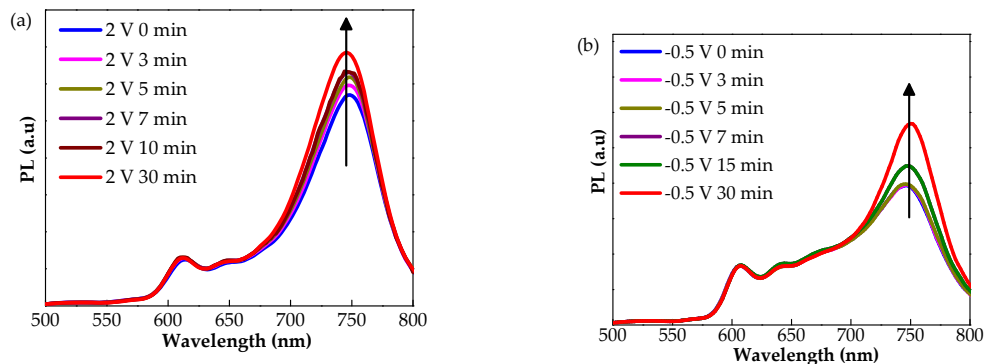


**Figure 7.** PL spectra of electric field modulated quasi-2D perovskite solar cells. (**a**) different modulation time at the forward bias of 2 V. (**b**) Different modulation time at the reversed bias of $-0.5$ V.

## 5. Conclusions

In summary, we report that the charge carrier transport can be manipulated by electric field modulation in quasi-2D perovskite solar cells. Using $V_{app} < V_{bi}$ with proper modulation time, the parameters of photovoltaics can be improved, which indicates that electric polarization formed by electric field modulation enhances charge carrier transport. When the forward bias $V_{app} > V_{bi}$ or reversed bias applied, the device performance was reduced. Furthermore, the quenching PL signal indicates that electric field modulation is responsible for charge carrier transport in quasi-2D perovskite solar cells. More importantly, we found that $\Delta PL/PL_0$ show obvious low $n$ value peak in the worse performance devices with improper electric field modulation. This further confirms that electric field modulation plays a crucial role for carrier transport in quasi-2D perovskites. The electric field modulation functioning as an effective experimental method to form fast charge transfer between quantum wells through electric polarization allows the charge carrier transport from low $n$

value nanoplates to high *n* value nanoplates to develop high-efficiency quasi-2D perovskite solar cells.

## References

1. Lee, J.-W.; Dai, Z.; Han, T.-H.; Choi, C.; Chang, S.-Y.; Lee, S.-J.; De Marco, N.; Zhao, H.; Sun, P.; Huang, Y.; et al. 2D perovskite stabilized phase-pure formamidinium perovskite solar cells. *Nat. Commun.* **2018**, *9*, 3021. [CrossRef]
2. Ma, C.; Shen, D.; Ng, T.-W.; Lo, M.-F.; Lee, C.-S. 2D Perovskites with short interlayer distance for high-performance solar cell application. *Adv. Mater.* **2018**, *30*, e1800710. [CrossRef]
3. Cohen, B.-E.; Wierzbowska, M.; Etgar, L. High efficiency and high open circuit voltage in quasi 2D perovskite based solar cells. *Adv. Funct. Mater.* **2016**, *27*, 1604733. [CrossRef]
4. Yang, W.S.; Park, B.-W.; Jung, E.H.; Jeon, N.J.; Kim, Y.C.; Lee, D.U.; Shin, S.S.; Seo, J.; Kim, E.K.; Noh, J.H.; et al. Iodide management in formamidinium-lead-halide–based perovskite layers for efficient solar cells. *Science* **2017**, *356*, 1376–1379. [CrossRef]
5. Ren, M.; Cao, S.; Zhao, J.; Zou, B.; Zeng, R. Advances and challenges in two-dimensional organic–inorganic hybrid per-ovskites toward high-performance light-emitting diodes. *Nano Micro Lett.* **2021**, *13*, 1–36. [CrossRef] [PubMed]
6. Liu, P.; Yu, S.; Xiao, S. Research progress on two-dimensional (2D) halide organic–inorganic hybrid perovskites. *Sustain. Energy Fuels* **2021**, *5*, 3950–3978. [CrossRef]
7. Zhang, L.; Sun, C.; He, T.; Jiang, Y.; Wei, J.; Huang, Y.; Yuan, M. High-performance quasi-2D perovskite light-emitting diodes: From materials to devices. *Light Sci. Appl.* **2021**, *10*, 61. [CrossRef] [PubMed]
8. Zhang, X.; Munir, R.; Xu, Z.; Liu, Y.; Tsai, H.; Nie, W.; Li, J.; Niu, T.; Smilgies, D.; Kanatzidis, M.G.; et al. Phase Transition Control for High Performance Ruddlesden–Popper Perovskite Solar Cells. *Adv. Mater.* **2018**, *30*, e1707166. [CrossRef] [PubMed]
9. Roghabadi, F.A.; Alidaei, M.; Mousavi, S.M.; Ashjari, T.; Tehrani, A.S.; Ahmadi, V.; Sadrameli, S.M. Stability progress of perovskite solar cells dependent on the crystalline structure: From 3D ABX3 to 2D Ruddlesden–Popper perovskite absorbers. *J. Mater. Chem. A* **2019**, *7*, 5898–5933. [CrossRef]
10. Wang, K.; Li, Z.; Zhou, F.; Wang, H.; Bian, H.; Zhang, H.; Wang, Q.; Jin, Z.; Ding, L.; Liu, S. Ruddlesden–Popper 2D Com-ponent to Stabilize γ-CsPbI3 Perovskite Phase for Stable and Efficient Photovoltaics. *Adv. Energy Mater.* **2019**, *9*, 1902529. [CrossRef]
11. Chen, Y.; Sun, Y.; Peng, J.; Tang, J.; Zheng, K.; Liang, Z. 2D Ruddlesden-Popper Perovskites for Optoelectronics. *Adv. Mater.* **2018**, *30*, 1703487. [CrossRef] [PubMed]

12.  Zheng, K.; Chen, Y.; Sun, Y.; Chen, J.; Chábera, P.; Schaller, R.; Al-Marri, M.J.; Canton, S.E.; Liang, Z.; Pullerits, T. Inter-phase charge and energy transfer in Ruddlesden–Popper 2D perovskites: Critical role of the spacing cations. *J. Mater. Chem. A* **2018**, *6*, 6244–6250. [CrossRef]
13.  Tsai, H.; Nie, W.; Blancon, J.-C.; Stoumpos, C.; Asadpour, R.; Harutyunyan, B.; Neukirch, A.J.; Verduzco, R.; Crochet, J.; Tretiak, S.; et al. High-efficiency two-dimensional Ruddlesden–Popper perovskite solar cells. *Nat. Cell Biol.* **2016**, *536*, 312–316. [CrossRef]
14.  Zhang, J.; Qin, J.; Wang, M.; Bai, Y.; Zou, H.; Keum, J.K.; Tao, R.; Xu, H.; Yu, H.; Haacke, S.; et al. Uniform Permutation of Quasi-2D perovskites by vacuum poling for efficient, high-fill-factor solar cells. *Joule* **2019**, *3*, 3061–3071. [CrossRef]
15.  Xiao, X.; Dai, J.; Fang, Y.; Zhao, J.; Zheng, X.; Tang, S.; Rudd, P.N.; Zeng, X.C.; Huang, J. Suppressed Ion Migration along the In-Plane Direction in Layered Perovskites. *ACS Energy Lett.* **2018**, *3*, 684–688. [CrossRef]
16.  Kim, H.; Kim, J.S.; Heo, J.-M.; Pei, M.; Park, I.-H.; Liu, Z.; Yun, H.J.; Park, M.-H.; Jeong, S.-H.; Kim, Y.-H. Proton-transfer-induced 3D/2D hybrid perovskites suppress ion migration and reduce luminance overshoot. *Nat. Commun.* **2020**, *11*, 3378. [CrossRef]
17.  Lin, Y.; Bai, Y.; Fang, Y.; Wang, Q.; Deng, Y.; Huang, J. Suppressed ion migration in low-dimensional perovskites. *ACS Energy Lett.* **2017**, *2*, 1571–1572. [CrossRef]
18.  Liu, P.; Wang, W.; Liu, S.; Yang, H.; Shao, Z. Fundamental understanding of photocurrent hysteresis in perovskite solar cells. *Adv. Energy Mater.* **2019**, *9*, 1803017. [CrossRef]
19.  Cheng, T.; Tumen-Ulzii, G.; Klotz, D.; Watanabe, S.; Matsushima, T.; Adachi, C. Ion migration-induced degradation and efficiency roll-off in quasi-2D perovskite light-emitting diodes. *ACS Appl. Mater. Interfaces* **2020**, *12*, 33004–33013. [CrossRef] [PubMed]
20.  Liu, F.; Wang, L.; Wang, J.; Wang, F.; Chen, Y.; Zhang, S.; Sun, H.; Liu, J.; Wang, G.; Hu, Y. 2D Ruddlesden–popper perovskite single crystal field-effect transistors. *Adv. Funct. Mater.* **2021**, *31*, 2005662. [CrossRef]
21.  Li, Z.; Xiao, C.; Yang, Y.; Harvey, S.P.; Kim, D.H.; Christians, J.A.; Yang, M.; Schulz, P.; Nanayakkara, S.U.; Jiang, C.-S.; et al. Extrinsic ion migration in perovskite solar cells. *Energy Environ. Sci.* **2017**, *10*, 1234–1242. [CrossRef]
22.  Zhang, J.; Chen, R.; Wu, Y.; Shang, M.-H.; Zeng, Z.; Zhu, Y.; Han, L. Extrinsic Movable Ions in MAPbI3 Modulate Energy Band Alignment in Perovskite Solar Cells. *Adv. Energy Mater.* **2017**, *8*, 1701981. [CrossRef]
23.  Leijtens, T.; Kandada, A.R.S.; Eperon, G.E.; Grancini, G.; D'Innocenzo, V.; Ball, J.M.; Stranks, S.D.; Snaith, H.J.; Petrozza, A. Modulating the electron–Hole interaction in a hybrid lead halide perovskite with an electric field. *J. Am. Chem. Soc.* **2015**, *137*, 15451–15459. [CrossRef]
24.  Hu, X.; Wang, X.; Fan, P.; Li, Y.; Zhang, X.; Liu, Q.; Zheng, W.; Xu, G.; Wang, X.; Zhu, X.; et al. Visualizing Carrier Transport in Metal Halide Perovskite Nanoplates via Electric Field Modulated Photoluminescence Imaging. *Nano Lett.* **2018**, *18*, 3024–3031. [CrossRef] [PubMed]
25.  Shi, J.; Xu, X.; Zhang, H.; Luo, Y.; Li, D.; Meng, Q. Intrinsic slow charge response in the perovskite solar cells: Electron and ion transport. *Appl. Phys. Lett.* **2015**, *107*, 163901. [CrossRef]
26.  Zhang, J.; Zhu, X.; Wang, M.; Hu, B. Establishing charge-transfer excitons in 2D perovskite heterostructures. *Nat. Commun.* **2020**, *11*, 2618. [CrossRef] [PubMed]
27.  Wu, G.; Li, X.; Zhou, J.; Zhang, J.; Zhang, X.; Leng, X.; Wang, P.; Chen, M.; Zhang, D.; Zhao, K.; et al. Fine Multi-Phase Alignments in 2D Perovskite Solar Cells with Efficiency over 17% via Slow Post-Annealing. *Adv. Mater.* **2019**, *31*, e1903889. [CrossRef] [PubMed]
28.  Eames, C.; Frost, J.M.; Barnes, P.; O'Regan, B.C.; Walsh, A.; Islam, M.S. Ionic transport in hybrid lead iodide perovskite solar cells. *Nat. Commun.* **2015**, *6*, 7497. [CrossRef]
29.  De Bastiani, M.; Dell'Erba, G.; Gandini, M.; D'Innocenzo, V.; Neutzner, S.; Kandada, A.R.S.; Grancini, G.; Binda, M.; Prato, M.; Ball, J.M. Ion migration and the role of preconditioning cycles in the stabilization of the J–V characteristics of inverted hybrid perovskite solar cells. *Adv. Energy Mater.* **2016**, *6*, 1501453. [CrossRef]
30.  Hoke, E.T.; Slotcavage, D.J.; Dohner, E.R.; Bowring, A.R.; Karunadasa, H.I.; McGehee, M.D. Reversible photo-induced trap formation in mixed-halide hybrid perovskites for photovoltaics. *Chem. Sci.* **2015**, *6*, 613–617. [CrossRef]
31.  Fabregat-Santiago, F.; Garcia-Belmonte, G.; Mora-Seró, I.; Bisquert, J. Characterization of nanostructured hybrid and organic solar cells by impedance spectroscopy. *Phys. Chem. Chem. Phys.* **2011**, *13*, 9083–9118. [CrossRef]
32.  Zhu, X.; Wang, K.; Zhao, F.; Han, C.; Yang, Q.; Yu, H.; Zhang, F.; Hu, B. Revisiting the Impact of Interfacial Transport Layers on Organic Bulk Heterojunction Systems. *ACS Appl. Energy Mater.* **2018**, *1*, 3457–3468. [CrossRef]
33.  Lin, Y.; Fang, Y.; Zhao, J.; Shao, Y.; Stuard, S.J.; Nahid, M.M.; Ade, H.; Wang, Q.; Shield, J.E.; Zhou, N. Unveiling the operation mechanism of layered perovskite solar cells. *Nat. Commun.* **2019**, *10*, 1008. [CrossRef] [PubMed]
34.  Zhu, X.; Xu, H.; Liu, Y.; Zhang, J.; Wang, M.; Ivanov, I.N.; Ovchinnikova, O.S.; Hu, B. Two-Photon Up-conversion photoluminescence realized through spatially extended gap states in Quasi-2D perovskite films. *Adv. Mater.* **2019**, *31*, 1901240. [CrossRef] [PubMed]